Journal of Engineering Mathematics **25**: 63–75, 1991.
© 1991 *Kluwer Academic Publishers. Printed in the Netherlands.*

Slowly moving hull forms in short waves

A.J. HERMANS

Department of Applied Mathematics and Computer Science, Delft University of Technology, P.O. Box 356, 2600 AJ Delft, The Netherlands

Received 18 December 1989; accepted in revised form 5 April 1990

Abstract. The purpose of this paper is to provide a mathematical tool to improve the optimal design of ship forms. It is common practice that hull forms are designed such that they have minimum wave resistance in calm water. In this paper a theory is described by which the effect of short waves may be incorporated.

The basic tool we use is the ray theory. First, the appropriate free-surface condition is shown. Then, the standard ray method, well-known in geometric optics, is formulated in the fluid region and at the free surface. After an elimination process the eiconal equation and the transport equation are obtained. The characteristic equation for the nonlinear eiconal equation is derived, keeping in mind that the characteristics are not perpendicular to the wave fronts, due to the effect of the double-body potential due to the forward speed of the ship, which is assumed to be a good approximation for the steady potential.

Numerical computations are carried out by means of the RK4 method to obtain the ray pattern. After some manipulations the amplitude may be computed just as well. Finally, the nonlinear added-resistance force is calculated. Pictures of ray patterns for several angles of incidence are shown. Also the forces are shown.

1. Introduction

It is common practice that hull forms are designed such that they have minimum wave resistance in calm water. As has been noticed by Sakamoto and Baba [1] it is worthwhile to take added resistance due to waves into account as well. Large ships, sailing in an average sea state, encounter mainly waves that are short compared with the ship length. Moreover, ship motions for these short waves are negligible, while the value of the added resistance is not small compared to the wave resistance in calm water. It is found that this is true for all wave directions, not only for general ship forms, but also for symmetric bodies such as ellipsoids. It has been shown [1] that optimal forms can be designed by taking the added resistance into account. However, the approximations used are questionable. The formulation of Faltinsen's [2] approximate solution is different from the one presented by Sakamoto and Baba [1]. For a thorough discussion we refer to the latter authors.

In this paper a theory is presented that is valid for ships sailing in short waves. Numerical computations are carried out for some simple hull shapes, such as a surface-piercing vertical circular cylinder and a sphere, for several wave directions. The basic equations for a slowly moving ship in short waves have been derived in [1]. Here we indicate the major steps and arrive at the final formulation.

The next step is to derive a short-wave theory valid in the whole field. It turns out that a direct application of the ray theory is possible. The eiconal equation for the phase function is obtained together with a transport equation for the amplitude function. The characteristics of the eiconal equations are computed. Along these characteristics, the differential equation for the amplitude function is solved. The Neumann condition at the hull is used to describe the reflection of the waves. Finally, the added resistance is computed by an averaged-pressure integration along the wetted hull.

2. Free surface condition

The ship is sailing in short waves. The motion of the ship due to these short waves is neglected throughout this paper and the coordinate system is fixed to the body (see Fig. 1). The undisturbed free surface is at $z = 0$.

The fluid is assumed to be inviscid and incompressible. The flow is irrotational. Hence, we introduce the velocity potential $\Phi(\mathbf{x}, t)$ as $\mathbf{u}(\mathbf{x}, t) = \text{grad}\,\Phi(\mathbf{x}, t)$ where $\mathbf{u}(\mathbf{x}, t)$ is the fluid velocity. The equation for the total potential function Φ can be written as

$$\Delta\Phi = 0 \quad \text{in the fluid} . \tag{1}$$

The free-surface elevation is defined as $z = \zeta(x, y, t)$. At the free surface we have the dynamic and kinematic boundary condition,

$$\left.\begin{aligned} g\zeta + \Phi_t + \tfrac{1}{2}\nabla\Phi\cdot\nabla\Phi &= \tfrac{1}{2}U^2 \\ \Phi_z - \Phi_z\zeta_x - \Phi_y\zeta_y - \zeta_t &= 0 \end{aligned}\right\} \quad \text{at } z = \zeta(x, y, t) . \tag{2}$$

Elimination of ζ leads to the following nonlinear condition,

$$\frac{\partial^2\Phi}{\partial t^2} + g\frac{\partial\Phi}{\partial z} + \frac{\partial}{\partial t}(\nabla\Phi\cdot\nabla\Phi) + \nabla\Phi\cdot\nabla\left(\frac{\nabla\Phi\cdot\nabla\Phi}{2}\right) = 0 \quad \text{at } z = \zeta(x, y, t) . \tag{3}$$

Once the potential function Φ is determined the surface elevation may be computed by means of the dynamic boundary condition. The potential $\Phi(\mathbf{x}, t)$ is split up into the following three components:

$$\Phi(\mathbf{x}, t) = \phi_r(\mathbf{x}) + \phi_0(\mathbf{x}) + \phi(\mathbf{x}, t) ,$$

where ϕ_r represents the double-body flow in calm water, ϕ_0 is the steady wave potential and ϕ is the unsteady wave potential. The Froude number, defined with respect to the ship length L, $F = U/\sqrt{gL}$, is assumed to be small. In this situation, Sakamoto and Baba [1] obtain after the coordinate transformation

$$x' = x , \qquad y' = y , \qquad z' = z - \zeta_r(x, y)$$

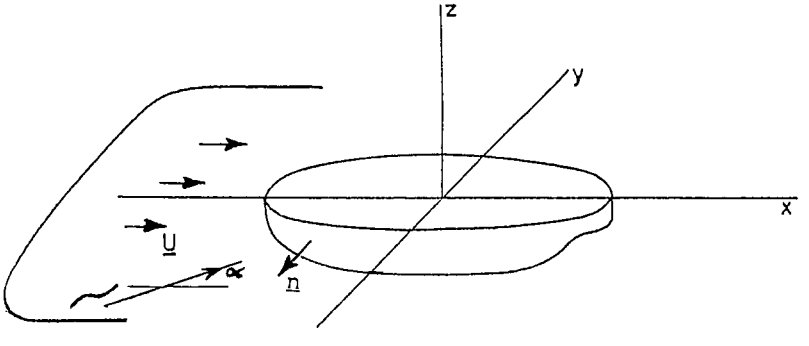

Fig. 1. Coordinate system.

the following boundary condition for the unsteady wave potential $\phi(\mathbf{x}, t)$, after omitting primes,

$$\frac{1}{g}\left[\frac{\partial}{\partial t} + u\frac{\partial}{\partial x} + v\frac{\partial}{\partial y}\right]^2 \phi + \frac{\partial}{\partial z}\phi = 0 \quad \text{on } z = 0\,, \tag{4}$$

where ζ_r is the free-surface elevation due to ϕ_r and the velocity $\mathbf{u} = \text{grad}\ \phi_r$ is calculated at the undisturbed free surface. This free-surface condition is valid if ϕ_t and $\mathbf{u}\cdot\nabla\phi$ are of the same order of magnitude. Furthermore, the terms $(1/g)\phi_{tt}$ and ϕ_z must be of the same order. This is the case if the frequency of the waves is large, while the dimensionless parameter $\tau = \omega U/g$ remains finite. It has been shown in [1] that the terms neglected in (2) are small in this situation.

For a discussion of the free-surface condition for ϕ_0 we refer to Eggers [3], Hermans and Brandsma [4] and Hermans and Van Gemert [5]. In this paper we are concerned with the unsteady potential ϕ.

3. Approximate theories

In the literature several asymptotic results are given to compute the added resistance. Faltinsen et al. [2] have derived an elegant theory, based on the assumption that the body is slender or thin. In this theory, the time-averaged value of the lateral force, the added resistance in short waves, is given by (in the notation of [1])

$$R_{aw} = \int_{\text{WL}} \bar{F}_n \sin\theta\, \mathrm{d}l\,, \tag{5}$$

$$\bar{F}_n = \frac{1}{4}\rho g \zeta_a^2 \left[\frac{k_1}{k_0} - \cos^2(\theta+\alpha) + \frac{k_2}{k_0}\sin(\theta+\alpha)\right], \tag{6}$$

with

$$k_1 = \{\omega - Vk_0\cos(\theta+\alpha)\}^2/g\,, \tag{7}$$

$$k_2 = \{k_1^2 - k_0^2\cos^2(\theta+\alpha)\}^{\frac{1}{2}}\,, \tag{8}$$

where $\bar{F}_n$ is the wave force acting on an infinitesimally small vertical element of the hull, $\omega = \omega_0 + k_0 U\cos\alpha$ is the circular frequency of encounter, k_0 and ζ_a are wave number and amplitude of the incident wave, $\alpha = \pi - \chi$ is the wave direction and θ is the inclination of the waterline, V is the velocity along the streamline. The integration in (5) is performed along the water line WL.

The diffracted wave is assumed to be of the form

$$\phi_D = A\,\mathrm{e}^{-\mathrm{i}\omega t}\exp[k_1 z + \mathrm{i}\{k_0 s\cos(\theta+\alpha) - nk_2\}]\,, \tag{9}$$

where n and s are coordinates normal and tangent to the waterline in the non-shadow part of the wave region.

The low-speed limit for $\bar{F}_n$ becomes

$$\bar{F}_n = \frac{1}{2}\rho g\zeta_a^2\left[\sin^2(\theta+\alpha) + 2\frac{\omega_0 U}{g}\{1-\cos\theta\cos(\theta+\alpha)\}\right], \tag{10}$$

where the approximation $V = U\cos\theta$ has been used. Sakamoto and Baba [1] arrive at a slightly different expression, namely

$$\bar{F}_n = \frac{1}{2}\rho g\zeta_a^2\left[\sin^2(\theta+\alpha) + 2\frac{\omega_0 U}{g}\{\cos\alpha-\cos\theta\cos(\theta+\alpha)\}\right]. \tag{11}$$

Now we consider the case of a surface-piercing vertical circular cylinder. We keep in mind that this out of the range of the asymptotic assumptions made by Faltinsen et al. in their derivation. Therefore, the results need not be reliable, a priori. In this case, the integration can be carried out analytically. Faltinsen's formula then becomes

$$R_{aw} = \frac{1}{2}\rho g\zeta_a^2\left[\frac{4}{3}\left\{\cos\alpha + \frac{\omega_0 U}{g}(1+\cos^2\alpha)\right\}\right]. \tag{12}$$

Sakamoto and Baba [1] state that the exact result $V = 2U\cos\theta$ can be used instead of the thin-ship approximation $V = U\cos\theta$. In this case a good candidate for the added resistance is provided by the expression

$$R_{aw} = \frac{1}{2}\rho g\zeta_a^2\left[\frac{4}{3}\left\{\cos\alpha + \frac{\omega_0 U}{g}(1+\sin^2\alpha)\right\}\right]. \tag{13}$$

They also state that, due to evanescent wave modes along the hull, their results may lead to an overestimation. In the next section we derive results in the short-wave case without the geometric restrictions of [1] and [2].

4. The ray method

The time dependent potential $\phi(\mathbf{x}, t)$ has to be a solution of

$$\Delta\phi = 0 \quad \text{in the fluid}, \tag{14}$$

$$\frac{1}{g}\left[\frac{\partial}{\partial t} + u\frac{\partial}{\partial x} + v\frac{\partial}{\partial y}\right]^2\phi + \frac{\partial\phi}{\partial z} = 0 \quad \text{on } z = 0, \tag{15}$$

$$\frac{\partial\phi}{\partial n} = 0 \quad \text{on the ship's hull}. \tag{16}$$

At infinity the incoming wave field consists of plane waves,

$$\phi_{\text{inc}} = e^{ik_0(x\cos\alpha + y\sin\alpha) - i\omega t}, \tag{17}$$

where $k_0 = \omega_0^2/g$ for deep water and $\omega = \omega_0 + k_0 U\cos\alpha$ is the relative frequency. We consider short waves with respect to the ship length L, i.e. $k_0 L = \omega_0^2 L/g \gg 1$. However, it is more convenient to choose $k = \omega^2/g$ as the large parameter.

We introduce the ray expansion

$$\phi(\mathbf{x}, t; k) = a(\mathbf{x}, k)\, \mathrm{e}^{\mathrm{i}kS(\mathbf{x})-\mathrm{i}\omega t}\,, \tag{18}$$

where $S(\mathbf{x})$ is the phase function and $a(\mathbf{x}, k)$ the amplitude function. The latter is written as a regular series expansion with respect to inverse powers of $\mathrm{i}k$,

$$a(\mathbf{x}, k) = \sum_{j=0}^{N} \frac{a_j(\mathbf{x})}{(\mathrm{i}k)^j} + \mathrm{o}((\mathrm{i}k)^{-N})\,. \tag{19}$$

Our aim, in this paper, is to determine $S(\mathbf{x})$ and $a_0(\mathbf{x})$.

Insertion of (18) into the Laplace equation (14) gives

$$-k^2\nabla_3 S\cdot\nabla_3 S a + \mathrm{i}k(2\nabla_3 a\cdot\nabla_3 S + a\Delta_3 S) + \mathrm{O}(1) = 0\,. \tag{20}$$

The subscript 3 is used to indicate the three-dimensional ∇ and Δ operator. If no subscript is used the operator is two-dimensional in the horizontal plane. Comparing orders of magnitude in (20) leads to a set of equations for S and a_0 to be satisfied in the fluid region:

$$\mathrm{O}(k^2)\colon\quad \nabla_3 S\cdot\nabla_3 S = 0\,, \tag{21}$$

$$\mathrm{O}(k^1)\colon\quad 2\nabla_3 a_0\cdot\nabla_3 S + a_0\Delta_3 S = 0\,. \tag{22}$$

Next we insert (18) into the free-surface condition (15) and obtain

$$\begin{aligned}&-k^2\{1-\mathbf{u}\cdot\nabla S)^2 - \mathrm{i}S_z\}a - \mathrm{i}k\{2\mathbf{u}\cdot\nabla a - 2(\mathbf{u}\cdot\nabla S)(\mathbf{u}\cdot\nabla a)\\ &-\mathbf{u}\cdot\nabla(\mathbf{u}\cdot\nabla S)a + \mathrm{i}a_z\} + \mathrm{O}(1) = 0\,.\end{aligned} \tag{23}$$

Comparing orders of magnitude in (23) yields

$$\left.\begin{aligned}&\mathrm{O}(k^2)\colon\quad \mathrm{i}S_z = (1-\mathbf{u}\cdot\nabla S)^2 &(24)\\ &\mathrm{O}(k^1)\colon\quad a_{0z} = \mathrm{i}\{2\mathbf{u}\cdot\nabla a_0 - 2(\mathbf{u}\cdot\nabla\mathrm{S})(\mathbf{u}\cdot\nabla a_0) - \mathbf{u}\cdot\nabla(\mathbf{u}\cdot\nabla S)a_0\} &(25)\end{aligned}\right\}\quad \text{at } z = 0\,.$$

The equation for the phase function at the free surface is obtained by elimination of S_z. Equations (21) and (24) yield the eiconal equation

$$(1-\mathbf{u}\cdot\nabla S)^4 - \nabla S\cdot\nabla S = 0\,, \tag{26}$$

while (22) and (25) yield the transport equation

$$[2\nabla S + 4(1-\mathbf{u}\cdot\nabla S)^3\mathbf{u}]\cdot\nabla a_0 + a_0 MS = 0\,, \tag{27}$$

where $MS = \Delta_3 S - 2\mathbf{u}\cdot\nabla(\mathbf{u}\cdot\nabla S)(1-\mathbf{u}\cdot\nabla S)^2$.

In order to solve the eiconal equation (26) we introduce the notation $S_x = p$, $S_y = q$, $\mathbf{p} = (p, q)$, write (26) in the standard form $F(x, y, S, p, q) = 0$ and apply the method of characteristics. The equation for the characteristics are the Charpit–Lagrange equations

$$\begin{aligned}
\frac{\mathrm{d}x}{\mathrm{d}\sigma} &= F_p = -4(1-\mathbf{u}\cdot\mathbf{p})^3 u - 2p\,, \\
\frac{\mathrm{d}y}{\mathrm{d}\sigma} &= F_q = -4(1-\mathbf{u}\cdot\mathbf{p})^3 v - 2q\,, \\
\frac{\mathrm{d}p}{\mathrm{d}\sigma} &= -(F_x + pF_S) = 4(1-\mathbf{u}\cdot\mathbf{p})^3(\mathbf{u}_x\cdot\mathbf{p})\,, \\
\frac{\mathrm{d}q}{\mathrm{d}\sigma} &= -(F_y + qF_S) = 4(1-\mathbf{u}\cdot\mathbf{p})^3(\mathbf{u}_y\cdot\mathbf{p})\,.
\end{aligned} \tag{28}$$

The characteristic curves, which are solutions of these equations, are called "rays", as in geometric optics. The phase function is obtained by solving the equation

$$\frac{\mathrm{d}S}{\mathrm{d}\sigma} = pF_q + qF_q = -4(1-\mathbf{u}\cdot\mathbf{p})^3 + 2\mathbf{p}\cdot\mathbf{p}\,. \tag{29}$$

The rays defined this way are not curves perpendicular to the wave fronts S = constant. The transport equation along the rays becomes

$$\frac{\mathrm{d}a_0}{\mathrm{d}\sigma} = a_0 MS\,. \tag{30}$$

To solve (28)–(30) we need initial conditions in the far field for the incident field and boundary conditions at the hull for the reflected field. We restrict ourselves to hull shapes that are perpendicular to the water surface at the waterline. To simplify the computations we restrict ourselves also to shapes with an analytic double-body solution, such as a circular cylinder, a sphere or elliptic cylinder. In the far field we consider plane waves $S(\mathbf{x})$ = constant = S_0 along a line L: $ax + by = c$, where c is chosen large enough. The initial conditions are found as follows. Along L the condition $S(x, y)$ = constant yields after differentiation a relation between p and q along L,

$$bp = aq\,. \tag{31}$$

Equations (31) and (26) yield the required initial conditions for p and q.

To compute the initial condition for the reflected waves, use is made of the boundary condition at the object. The boundary condition has to be obeyed by the superposition of the incident field and the reflected field,

$$\phi(\mathbf{x}, t) = a^{(i)}(\mathbf{x}, k)\,\mathrm{e}^{\mathrm{i}kS^{(i)}(\mathbf{x})-\mathrm{i}\omega t} + a^{(r)}(\mathbf{x}, k)\,\mathrm{e}^{\mathrm{i}kS^{(r)}(\mathbf{x})-\mathrm{i}\omega t}\,. \tag{32}$$

The boundary condition $\partial\phi/\partial n = 0$ yields

$$\begin{aligned}
&\{\mathrm{i}ka^{(i)}(\mathbf{n}\cdot\nabla S^{(r)}) + n\cdot\nabla a^{(i)}\}\,\mathrm{e}^{\mathrm{i}kS^{(i)}-\mathrm{i}\omega t} \\
&\quad = -\{\mathrm{i}ka^{(r)}(\mathbf{n}\cdot\nabla S^{(r)}) + \mathbf{n}\cdot\nabla a^{(r)}\}\,\mathrm{e}^{\mathrm{i}kS^{(r)}-\mathrm{i}\omega t}\,,
\end{aligned} \tag{33}$$

from which follows

$$S^{(r)}(\mathbf{x}) = S^{(i)}(\mathbf{x}) \quad \text{at the object}\,, \tag{34}$$

and

$$a_0^{(r)}(\mathbf{x}) = -a_0^{(i)}(\mathbf{x}) \frac{\mathbf{n} \cdot \nabla S^{(i)}}{\mathbf{n} \cdot \nabla S^{(r)}} \quad \text{at the object .} \tag{35}$$

Relation (34) is the initial condition for the reflected rays (Fig. 2).

The waterline is given $\mathbf{x} = \mathbf{x}(\tau)$. We then obtain, after differentiation of (34) with respect to τ,

$$\nabla S^{(r)} \cdot \mathbf{t} = \nabla S^{(i)} \cdot \mathbf{t} , \tag{36}$$

where $\mathbf{t}$ is the vector tangent to the curve at the point of interception. The vector $\mathbf{p} = \nabla S$ is the vector normal to the wave front $S = \text{constant}$. Therefore, we may say that the normal to the wave front obeys Snellius' reflection law at the interface. The rays do not coincide with the normal to the wavefront as follows from the first two equations in (28). We assume that $\nabla S^{(i)} \cdot \mathbf{t}$ is computed by the integration of (28) up to the surface, then (36) is a relation between the initial values of p and q for the reflected rays. The second relation is the eiconal equation. Hence, p and q are known explicitly at the waterline. Integration of (28) yields the reflected rays. The integration method used is RK4 which turns out to be a stable procedure for these ordinary differential equations. The next step is to compute the amplitude along the rays. Finally, we are interested in the amplitude of the incident and reflected waves at the waterline, because, as soon as the potential function is known, the second-order added resistance can be computed by means of a pressure integration along the hull.

Integration of (30) is relatively simple; we can write

$$a_0(\sigma) = a_0(\sigma_0) \exp\left\{ \int_{\sigma_0}^{\sigma} MS \, \mathrm{d}\sigma \right\} , \tag{37}$$

where $a_0(\sigma)$ is the initial value of the amplitude. The function MS, however, contains, among others, derivatives with respect to the vertical coordinate z. These terms can be handled by means of (24) and differentiation of (24). Finally, we obtain

$$\begin{aligned} MS = {} & S_{xx} \left\{ 1 - 2|\nabla S| u^2 - \frac{S_x^2}{S_x^2 + S_y^2} \right\} \\ & + S_{xy} \left\{ -4|\nabla S| uv - 2 \frac{S_x S_y}{S_x^2 + S_y^2} \right\} \\ & + S_{yy} \left\{ 1 - 2|\nabla S| v^2 - \frac{S_y^2}{S_x^2 + S_y^2} \right\} - 2|\nabla S| \nabla(\mathbf{u} \cdot \mathbf{u}) \cdot \nabla S . \end{aligned} \tag{38}$$

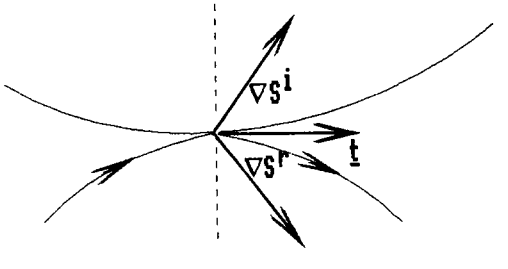

Fig. 2. Reflection of rays.

The terms $p = S_x$, $q = S_y$ are known along the rays. The terms S_{xx}, S_{xy} and S_{yy} must be computed with care. From the characteristic equations we have

$$S_{xx}\frac{dx}{d\sigma} + S_{xy}\frac{dy}{d\sigma} = \frac{dp}{d\sigma}, \tag{39}$$

where $dx/d\sigma$, $dy/d\sigma$, $dp/d\sigma$ are expressed in known functions by means of (28).

A second relation for S_{xx} and S_{xy} can only be obtained by means of numerical differentiation of values of S_x along neighbouring rays, see Fig. 3.
We take σ = constant and write

$$\Delta p = S_{xx}\,\Delta_x + S_{xy}\,\Delta y \tag{40}$$

where $\Delta f = f(i, j+1) - f(i, j)$. Then (39) and (40) yield

$$S_{xx} = \frac{\Delta p\, y_\sigma - p_\sigma\, \Delta y}{\Delta x\, y_\sigma - x_\sigma\, \Delta y}, \tag{41}$$

$$S_{xy} = \frac{\Delta p\, x_\sigma - p_\sigma\, \Delta x}{\Delta y\, x_\sigma - y_\sigma\, \Delta x}. \tag{42}$$

We also find

$$S_{yy} = \frac{q_\sigma - S_{xy}x_\sigma}{y_\sigma} = \frac{\Delta q\, x_\sigma - q_\sigma\, \Delta x}{\Delta y\, x_\sigma - y_\sigma\, \Delta x}. \tag{43}$$

Good results are obtained with the first part of (43), as long as y_σ is not close to zero.

The amplitude of the incident waves is computed according to (35). The amplitude of the reflected wave at the object is computed by means of (35). To compute the forces no further integration of the reflected amplitude is carried out. Looking at the computed ray patterns one may hardly expect that the amplitude of the reflected wave can be computed by means of (35) with sufficient accuracy. The numerical differentiation in MS leads to large errors if the rays diverge too much.

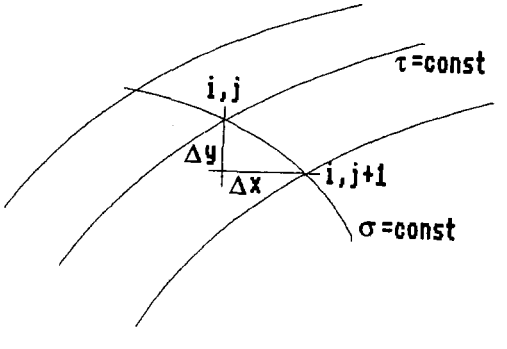

Fig. 3. Numerical differentiation.

5. The added resistance

The mean resistance $\mathbf{F}_{aw}$ is defined as the time-averaged force acting on the hull, due to waves. The force in the x-direction is the added resistance. In our case both the x and y component may be obtained. In general, we have

$$\mathbf{F}_{aw} = -\overline{\int_{z=-\infty}^{\zeta} \int_{\mathrm{WL}} p\mathbf{n}\,\mathrm{d}l\,\mathrm{d}z}\,, \tag{44}$$

where WL is the waterline and the bar indicates that the force is averaged with respect to time. The pressure p follows from Bernoulli's theorem,

$$-\frac{1}{\rho}(p - p_0) = \phi_t + \nabla_3\phi_r \cdot \nabla_3\phi + \frac{1}{2}\nabla_3\phi \cdot \nabla_3\phi + gz\,. \tag{45}$$

Again, the influence of the steady wave potential $\phi_0(\mathbf{x})$ is neglected in this expression. Inserting (45) into (44) leads to the expression for the steady second-order force

$$\mathbf{F}_{aw} = -\int_{\mathrm{WL}} \frac{1}{2}\rho g\zeta^2 \mathbf{n}\,\mathrm{d}l - \int_{S_0}\int \left\{-\frac{1}{2}\rho\nabla_3\phi \cdot \nabla_3\phi\right\}\mathbf{n}\,\mathrm{d}s\,, \tag{46}$$

where S_0 is the wetted surface in still water and $\zeta = -(\phi_t + \mathbf{u}\cdot\nabla\phi)/g$. Combining (32) and (46) leads to the following expression for the mean force

$$\begin{aligned}\mathbf{F}_{aw} = &-\frac{1}{4}k\rho\int_{\mathrm{WL}}[(\nabla S^{(i)}\cdot\nabla S^{(i)})^{\frac{1}{4}}a_0^{(i)} + (\nabla S^{(r)}\cdot\nabla S^{(r)})^{\frac{1}{4}}a_0^{(r)}]^2\,\mathbf{n}\,\mathrm{d}l \\ &+\frac{1}{4}k\rho\int_{\mathrm{WL}}\Bigg[a_0^{(i)^2}|\nabla S^{(i)}| + a_0^{(r)^2}|\nabla S^{(r)}| \\ &+ 2a_0^{(i)}a_0^{(r)}\frac{(\nabla S^{(i)}\cdot\nabla S^{(r)} + |\nabla S^{(i)}||\nabla S^{(r)}|)}{|\nabla S^{(i)}| + |\nabla S^{(r)}|}\Bigg]\mathbf{n}\,\mathrm{d}l\,.\end{aligned} \tag{47}$$

The numerical ray tracing gives all the terms in the integral. Hence, the mean force may be computed now and compared with the results of the approximate theories (12) and (13).

6. Results and discussion

First, the results are shown for a vertical circular cylinder with radius equal to unity in waves and current. The computed ray patterns differ a lot if the parameters are changed. This is due to the fact that the local velocity has a significant effect on the local group velocity, not only on its magnitude, but also on its direction. We keep in mind that we carry out the computations with the exact dispersion relation describing the wave pattern at low Froude number and for short waves. Figure 4 shows the ray patterns for three values of the dimensionless parameter τ. The rays are generated in the direction of the positive x-axis. The wavefronts are parallel to the y-axis in the far field. Positive values of $\tau = U\omega/g$ correspond to a flow field in the positive x-direction. For positive values of τ one obtains a pattern of the reflected rays that tends to have a caustic if the parameter τ is large enough. For the

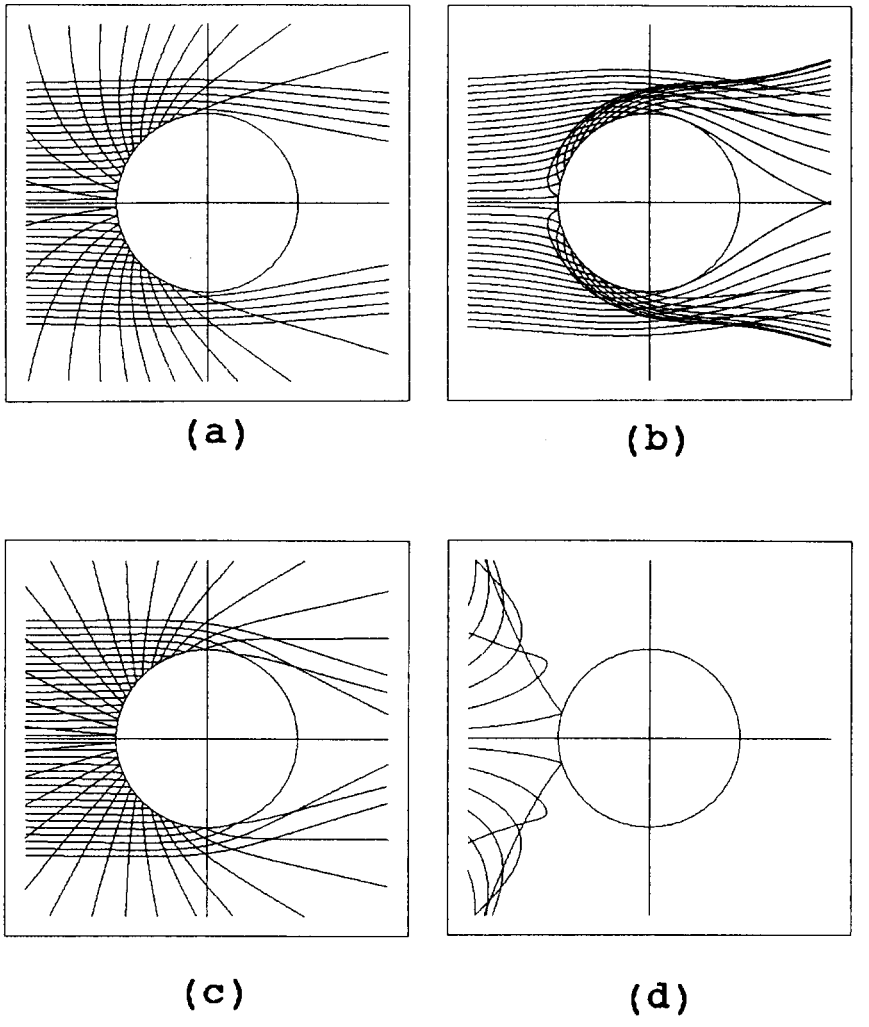

Fig. 4. Ray pattern for a circular cylinder with $\alpha = 0$: (a) $\tau = 0.25$, (b) $\tau = 1.0$, (c) $\tau = -0.1$, (d) $\tau = -0.25$.

relatively large value $\tau = 1$ the reflected pattern resembles the caustic behaviour of the Kelvin pattern of a ship sailing in still water.

However, for negative values of the parameter τ, that means that the flow is directed against the wavefield, the incident field shows caustics, and the amplitude can not be described by the methods of this paper. A uniformly valid expansion is needed near the caustic lines. In Fig. 5a the second-order added resistance is shown in comparison with the approximate results of Faltinsen et al. [2]. They give a very good correspondence for small values of τ, although the requirements for the approximate results to be reliable are not met. One cannot say that a circular cylinder looks like a thin body. The approximate results of Sakamoto and Baba [1] have a steepness near $\tau = 0$ half as large.

Figure 6 shows the ray pattern when the angle of incidence is $\pi/4$, for two values of the parameter τ. The mean surge and sway forces are shown in Fig. 5b. Here, the two approximate results for the force in the x-direction are the same, they both underestimate the added-resistance force.

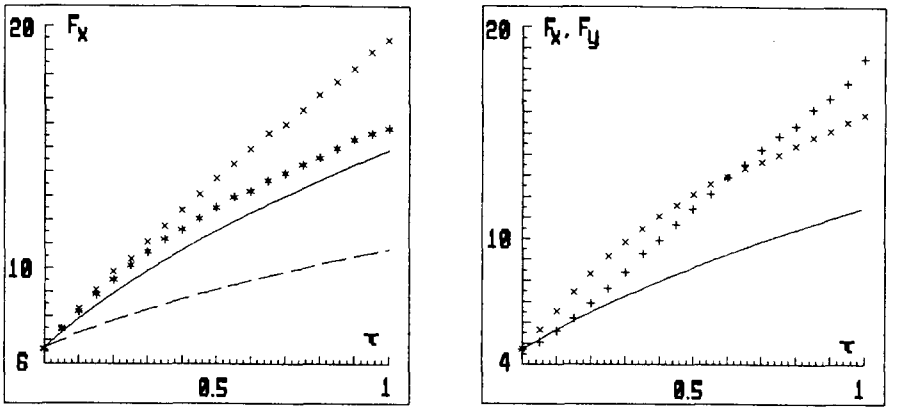

Fig. 5. (a) Added resistance $F_x = (\underline{F}_{aw})_x/\rho\zeta_a^2$, $\alpha = 0$, $\times\times\times$ circular cylinder, *** sphere, —— Faltinsen, – – – Sakamoto. (b) Circular cylinder, $\alpha = 45°$, $\times\times\times$ added resistance F_x, $+++$ mean sway force F_y, —— Faltinsen and Sakamoto (F_x).

Figure 8a shows the case where the wave fronts of the incident waves are parallel to the current. Again, it is seen that the double-body flow has great influence. Especially close to the cylinder, the rays are nearly parallel to the cylinder. This explains the rather small values of the mean force in the x-direction (Fig. 7a). The y-force (Fig. 7b) shows a more regular behaviour.

To get an idea of the influence of a three-dimensional double-body flow field, computations have been carried out for a sphere with the same radius as the circular cylinder. It is clear that the effect of the finite draft is not negligible, due to the changes of the flow field. Figure 8b shows an example of a ray pattern. The parameters are chosen to be the same as in Fig. 8a for the circular-cylinder case. The forces, shown in Fig. 9, are very different from the ones shown in Fig. 7. Again, it is remarkable that the approximate results of Faltinsen are very close to our computed results. In his computations no difference can be noticed in the x-forces acting on a circular cylinder or a sphere.

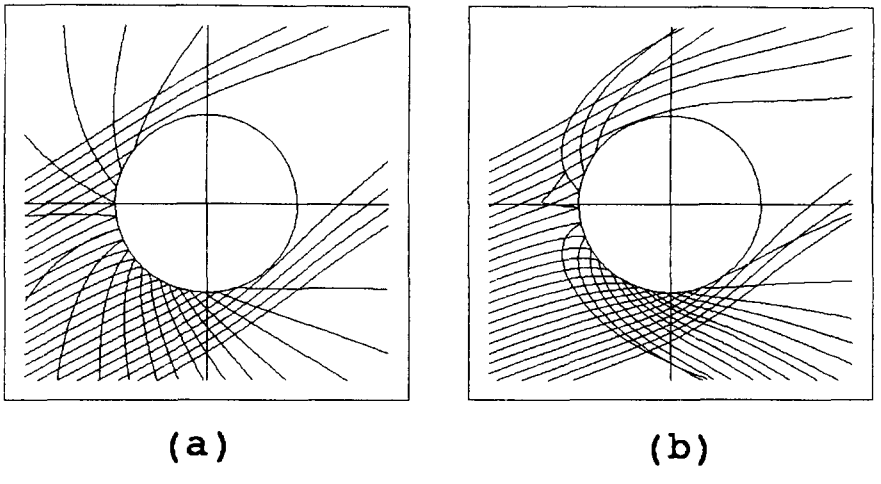

Fig. 6. Ray pattern for a circular cylinder with $\alpha = 45°$. (a) $\tau = 0.25$, (b) $\tau = 0.5$.

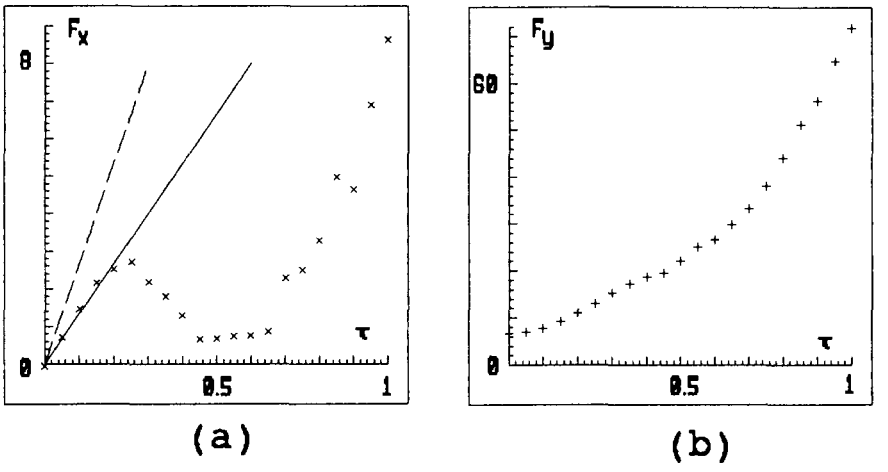

Fig. 7. Circular cylinder, $\alpha = 90°$. (a) $\times\times\times$ added resistance F_x, —— Faltinsen, – – – Sakamoto. (b) $+++$ mean sway force F_y.

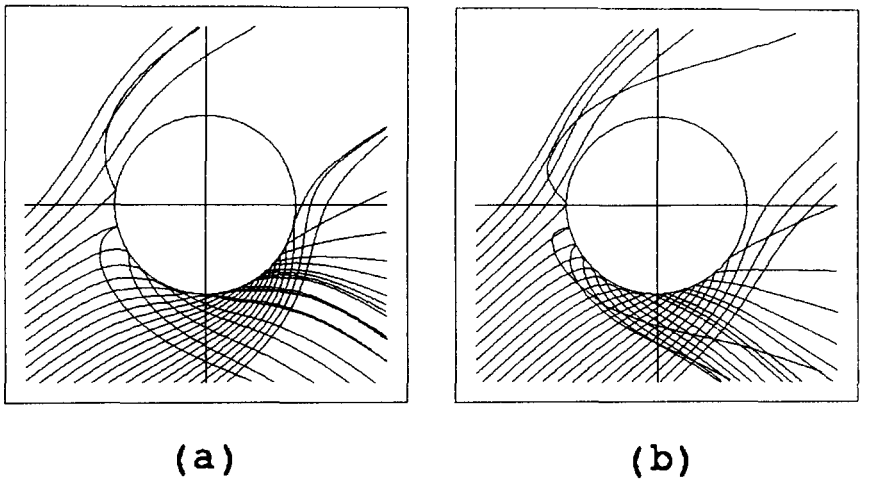

Fig. 8. Ray pattern for (a) a circular cylinder and (b) a sphere with $\alpha = 90°$ and $\tau = 0.5$.

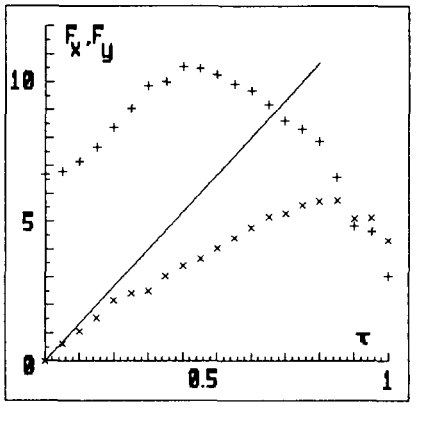

Fig. 9. Sphere, $\alpha = 90°$, $\times\times\times$ added resistance F_x, $+++$ mean sway force F_y, —— Faltinsen (F_x).

In conclusion, one can say that the computations, carried out by means of the ray method as described here, give reliable results for the second-order wave forces acting on bodies piercing the free surface vertically. In the case of a flow field and a field of short waves entering from the same half plane, results can be obtained over a wide range of parameters. Further investigations can be carried out in the situation where the incident wave field is forced by a double-body flow to generate caustics. A further extension to hull forms that are more general than the one described here, is possible in principle. In that case, a fast code must be available to compute the double-body velocity components and its derivatives in a large region around the ship.

The described method was motivated by the need to obtain tools for the optimal design of hull forms. The results are also of importance as the asymptotic limits for the calculation of the wave-drift damping as described by Huijsmans and Hermans [6] in their uniform method to describe the drift forces at low speed. In the high-frequency limit, as described here, the motion of the ship at the wave frequency is negligible, hence the second-order wave-drift force and the second-order added resistance are approximately the same.

References

1. Sakamoto, T. and Baba, E., Minimization of resistance of slowly moving full hull forms in short waves. *Proc. 16th Symposium on Naval Hydrodynamics*, Berkeley, USA (1986) 598–612.
2. Faltinsen, O.M., Minsaas, K.J., Liapis, N. and Skjordal, S.O., Prediction of resistance and propulsion of a ship in a sea way. *Proc. 13th Symposium on Naval Hydrodynamics*, Tokyo, Japan (1980) 505–529.
3. Eggers, K., Non-Kelvin dispersive waves around non-slender ships. *Schiffstechnik* 28 (1981) 223–251.
4. Hermans, A.J. and Brandsma, F.J., Nonlinear ship waves at low Froude number. *J. of Ship Research* 33 (1989) 176–193.
5. Hermans, A.J. and van Gemert, P.H., A linearized surface condition in low speed hydrodynamics. *Schiffstechnik* 36 (1989) 181–196.
6. Huijsmans, R.H.M. and Hermans, A.J., The effect of the steady perturbation potential on the motion of a ship sailing in random seas. *Proc. 5th Numerical Ship Hydrodynamics Conf.*, Hiroshima, Japan (1989).